FLOW PAST A BURNING SOLID SURFACE

Ramagopal Ananth (rananth@castor.nrl.navy.mil), Chuka C. Ndubizu[+],(cndubizu@castor.nrl.navy.mil, Geo Centers Inc., Lanham, MD) and Patricia.A. Tatem, Navy Technology Center for Safety & Survivability, Naval Research Laboratory, Washington, D.C., 20375 USA

ABSTRACT

Water mist suppression efficiency depends on local fluid dynamics and conditions at the fuel surface, which depend on geometry and the type of fuel. Solid fuels often form boundary layer flames, which have not been characterized fully even for the base case (without mist). In this work, detailed comparisons were made between steady state Navier-Stokes (NS) solutions, boundary layer theory, and our experimental data for PMMA for dimensionless regression rates, Nu, and dimensionless flame standoff distance. At short distances from the leading edge, xl, the results show that the computations agree with the data at short burn times. As the burn time is increased, the moving boundary effects due to change in the shape of the surface become increasingly important and the computations overpredict the data. At large values of xl, the results show good agreement between the steady state computations and the data for long burn times. The computations overpredict the data at short burn times. At large values of xl, the heat flux to the surface is small, and the regression rate increases with time due to transient heat conduction into the solid and approaches steady state values at long burn times. At a fixed value of Re, the computations predict increased Nu with increased air velocity U unlike the boundary layer (BL) theory, which predicts no change. This work also presents new PMMA data in which the burn time was varied.

INTRODUCTION

Studies on water mist suppression performed on ex USS Shadwell [1-3] have shown that water mist is a promising alternate to halon 1301. Most laboratory studies of suppression in flame temperature and burning rate, however, were performed for gaseous and liquid pool flames in co-flow [4-6] or counter-flow configurations. Solid fuels are often found in berthing space, laundry room, and other spaces on a ship and may respond differently from the gaseous or liquid fuels to water mist due to differences in the condensed phase pyrolysis and heat transfer. Indeed, the pyrolysis and heat transfer in solid materials occur over much longer time scales than for gaseous or even liquid fuels, due to lack of significant convection, and can be very complex. Therefore, a laboratory study was initiated to understand the mechanisms of burning and water mist suppression for boundary layer combustion of solid materials. In these studies often one must characterize the base case (without mist) before performing a suppression study. Despite a large body of literature on flame spread [7,8] on a PMMA surface, very little work has been performed on the burning or regression rate distribution for a non-spreading boundary layer flame formed under forced convection. Therefore, in this paper, we will present burning characteristics of a model polymer (polymethyl methacrylate, PMMA) for forced convection boundary layer flame for the base case (without mist).

In addition to flame spread on an object, understanding fully engulfed burning of an object is important since it relates to its potential to ignite other objects in the surrounding, and contribute to fire propagation across large spaces. Most laboratory scale studies of burning rates for polymeric solids were performed on vertical or horizontal plates under buoyancy driven flow conditions [9,10]. Forced convection offers a significant advantage in determining precisely the effects air flow velocity on the burning rates since the flow velocity can be varied independently. Most studies [7,8] that employ forced convection on burning fuel plates, however, were performed to study flame spread. They [7,8] report the rates of flame spread rather than the surface regression rate distributions underneath the flame. Furthermore, the change in surface regression with time is due both to unsteady transport of heat and spreading of the flame. In these studies, each point on the surface is exposed to different values of the heat feed back from the flame or for different periods of time, which are generally small, especially in co-currant spread. Therefore, a full understanding of the burning rate of materials may be obtained from non-spreading, forced convection, boundary layer flames formed by igniting the entire surface of the plate so that each point on the surface is exposed to the flame for the same period of time. The present study reports theoretical and experimental results on the non-spreading flame for different air velocities and burn times.

Emmons [11] obtained similarity solutions of the classical forced convection boundary layer equations, which neglect axial conduction and assume infinite rate combustion kinetics. He showed that the local burning rate or mass loss rate varies inversely with the square root of distance from the leading edge, xl, and directly with the square root of the air velocity, U. Sibulkin et al. [12] obtained similar solutions for buoyancy driven flow and included the effects of finite rate combustion kinetics. Unlike the classical similarity solutions, Chen and Tien [13] obtained solutions of the NS equations for unit Lewis Le Prandtl Pr and Schmidt Sc numbers for a small neighborhood (few mm @ U=100 cm/sec) near the leading edge. They, however, focused on flame "attachment" and showed the effect of decreasing Damkohler number Da on flame transition from a "closed" to an "open" flame. They provided solutions for small Reynolds number $Re_x = U(xl)/\nu < 300$ and estimated that $Re_x > 3000$ is needed to render the axial conduction terms negligible. Here, xl and ν are the distance from the leading edge and kinematic viscosity evaluated at the ambient temperature, respectively. Mao, Kodama, and Fernandez-Pello [14] presented NS solutions for mixed convection for thermal, concentration and velocity fields over a 5-cm length PMMA plate. Kodama, Miyasaka and Fernandez-Pello [15] calculated the effects of air flow velocity and oxygen mass fraction on extinction distance for the mixed convection boundary layer flame. They compared the predicted extinction lengths with those measured from diffusion flames formed by injecting heptane through a porous plate burner. In this work, we consider a configuration very similar to that studied by Kodama et al. [15] and obtain solutions for forced convection flames and for variable Le, Pr and Sc. We consider "open" flames and provide NS solutions up to $Re_x = 7000$, which is many times larger than that considered by Chen and Tien[13]. At the very leading edge, however, Re_x gets small ($Re_x<200$), and the NS solutions become less accurate due to grid size limitations. Unlike the previous studies, we provide discussion of burning rates and present detailed comparisons with both the PMMA experiments and the classical boundary layer theory. Furthermore, we consider the effects of finite rate pyrolysis kinetics, which vary significantly along the surface, and require iterative solutions at every cell along the surface, at each time step. The computations also include the effects of fully variable properties and realistic values of Pr, Sc and Le.

Flame spread on the surface of a PMMA plate has been studied widely by numerous investigators [16,17]. In these studies, the PMMA plate is at room temperature initially and is ignited at one end. The flame is allowed to spread as a result of heat transport to the solid surface *in front* of the flame front. The flame eventually spreads to the end of the plate within minutes and establishes a boundary layer flame in co-current flame spread experiment. These studies report rates of spread of a pyrolysis front in forced, co-current air flow past the surface. Very few of these studies [18,19], however, reported the solid surface regression rate distributions due to heat transport from the flame to the pyrolyzing solid *underneath*, which is the central focus of the present work. In these studies, the flame was allowed to spread to the end of the plate and the sample was allowed to burn subsequently for a long time. Zhou and Fernandez-Pello [18] showed that the dimensionless regression rate Nu increases as sqrt(Re) in qualitative agreement with Emmons solutions. Agrawal [19], on the other hand, reported that the regression rate varies as $xl^{-0.8}$ rather than $xl^{-0.5}$ expected from Emmons solutions. Therefore, the exact variation in regression rate underneath the flame with xl and U is not clear, since the main focus has been spreading in most of these studies. Especially not clear is the time dependent variation in the regression rate. We performed experiments to study heat transfer and pyrolysis under a non-spreading flame and varied the burn time, in addition to varying the air velocity [20-24].

In the present work, a non-spreading boundary layer flame was formed on a 10-cm length PMMA sample by exposing the entire sample surface to a radiant panel for a short period of time (~30 sec), igniting the vapors. The ignited sample is then quickly brought to a channel exit through which air is forced at a prespecified velocity to form the forced convection boundary layer flame. The sample is then allowed to burn at prespecified time and the flame is extinguished to measure the resulting regression in the sample surface as a function of distance from the leading edge. Regression rate profiles along the sample are measured for various burn times (2.5 to 20 min.) and at various air velocities (0.6 to 1.6 m/sec). The data exhibit significant transient effects due to change in the shape of the surface as a result of the moving boundary effects near the leading edge of the flame. There are also significant transient effects downstream due to solid phase phenomena. Since the samples are prepyrolysed, the surface is at the pyrolysis temperature prior to the experiment and transient burning is caused by in-depth transport in the solid phase. This is unlike flame spread or flameless pyrolysis [25] experiments performed under a radiant panel, where the sample surface is initially at room temperature.

APPROACH

Theoretical :

We consider air flow past a flat solid surface, which consists of a leading inert plate (1.7 cm), followed by a PMMA plate (6.5 cm), followed by another inert plate (8 cm) as shown in Figure 1. The solid surface is assumed to remain flat during combustion. Gases are ignited along the entire PMMA surface by adding external energy for a short period of time. Forced convection is assumed to dominate the buoyancy effects especially for a short distance from the leading edge, where we will show that the most burning occurs. The NS equations include radiation losses from the hot gases to the ambient following Stefan-Boltzman law. Methyl methacrylate

monomer vapor is assumed to undergo stochiometric combustion to form water vapor and carbon dioxide. A single-step, second-order, PMMA combustion kinetics given by Seshadri and Williams [26] is used (E = 43 Kcal/gmole, ΔH = 2530 KJ/gmole [27]). The solid polymer is assumed to undergo zeroth-order, single step pyrolysis at the surface to form the monomer vapor as shown by Arisawa and Brill [28] (E = 66000 cal/gmole, A = $8x10^{17}$ gm/cm^{2}sec). Effective diffusion coefficient D_{km}, of specie k is evaluated from binary diffusion coefficients and local mixture composition [29]. Similarly, viscosity μ_m conductivity λ_m and specific heat C_{pm} of the gas mixture are evaluated from pure specie values and the composition. The properties of n-pentane gas are used for the pure monomer vapor after correcting for the molecular weight difference. The NS equations are solved by using Barely Implicit Correction to Flux Corrected Transport (BIC-FCT) algorithms [30] with time-step splitting. The equations are discretized using 192 x 144 finite volume cells, with the smallest cells (0.2 mm x 0.2 mm) placed near the leading edge of the fuel plate. The cells are stretched at a low rate in both x and y directions from the leading edge.

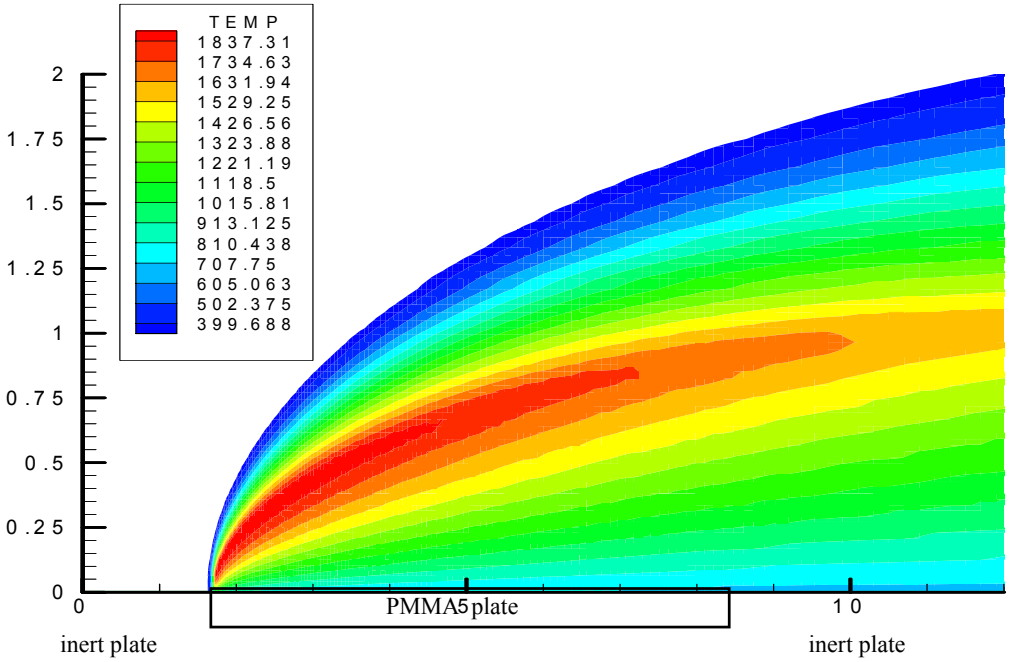

Figure 1 Navier-Stokes (NS) Solutions for Temperature Contours for U=60 cm/sec

A multi-variable fixed point iterative method was developed to implement the surface boundary conditions. Solution of the pyrolysis equation needs special attention. An implicit form of the pyrolysis equation was derived and was solved by Newton-Raphson iteration with bisection to obtain the new value of surface temperature,T_s. Thus, $\dot{m}$, X_k and T_s are iterated until convergence is achieved for every cell along the polymer surface, before proceeding to the next time step.

Experimental :

The solid plate is similar to that shown in Figure 1 in the experiments. The experimental set up was described elsewhere [20]. Thin quartz plates are placed all around the fuel plate to minimize excess burning of the edges. Also, extension plates (lip) are provided all around the fuel plate. Air is forced at a prespecified center velocity through a channel. A high-molecular-weight PMMA plate of 7.5 x 9.5 cm is ignited along the entire surface by placing it under a radiant panel for a short period of time. The ignited sample is brought to the exit of the channel, where a boundary layer flame is quickly formed on the horizontally placed fuel plate. After about 1 minute from the time of ignition, five fine thermocouples are brought into the flame to map the temperature profiles at different locations along the plate. During combustion, a thin film of melt is formed at the surface with intense bubbling near the leading edge and relatively slow bubbling far from the leading edge. The sample is allowed to burn for a given time before the flame is extinguished. Regression rate is the change in the thickness of the sample divided by the burn time and is measured at different distances from the leading edge of the plate [20-24]. The boundary layer formed is smooth except near the sides and near the trailing edge of the sample due to buoyancy effects. Measurements, however, are made well within the smooth region and along the center line of the sample.

RESULTS AND DISCUSSION

Solutions describe the temperature, specie mole fraction, velocity, and density profiles as functions of x, y, and t. Also, the values of $\dot{m}$, X_k and T_s along the surface are predicted. Our goal is to compare the computations with the data for burning rates and the classical Emmons solutions. These comparisons are made for dimensionless flame standoff distance and dimensionless regression rates. The computations and BL theory of Emmons are at steady state, while in the PMMA experiments, the burn time was varied.

Figure 1 shows typical temperature contours for inlet air velocity U of 60 cm/sec. The combustion reactions occur mostly in the high temperature region, which is represented by one of the dark bands. Near the leading edge, fresh fuel comes in contact with fresh air and the combustion rates are very high. The computations are expected to be valid at distances >1mm from the leading edge of the flame so that the grid size is much smaller than xl. Downstream, the products dilute the gases and the combustion rates decrease sharply with the distance from the leading edge. The rates of heat and mass transfer between the flame and the surface are also large near the leading edge due to steep gradients and they decrease with distance from the leading edge as the boundary layer thickness increases. Therefore, near the leading edge, the transport and combustion kinetics are expected to be closely coupled. Far from the leading edge, combustion rates are small and the transport dominates. Therefore, Damkohler number (reaction rate/flow rate) increases with distance from the leading edge, xl. Also, the axial gradients become smaller than the vertical gradients as xl increases. The classical boundary layer solutions given by Emmons are expected to apply at large Reynolds numbers, $Re=Uxl/\nu$, where ν is 0.157 cm^2/sec . The implications of the structure of transport and combustion phenomena on local regression rates are discussed below. In the following figures, the Reynolds number and the dimensionless regression rates are defined based on ambient properties so that the computations, theory and data can be compared on the same basis. The thermal conductivity λ that appears in the dimensionless regression rate, $Nu=(r0xlQ_p\rho_s)/(\lambda \Delta T)$, however, is defined based on the PMMA surface temperature, 700K. Here r0 is the regression rate, cm/sec; Q_p

(1.59×10^3 J/gm) is the heat of pyrolysis; ρ_s (1.19 gm/cm^3) is density of PMMA; λ (0.052 W/mK); ΔT=1200K.

Figure 2 shows that the NS solutions for the dimensionless flame standoff distance δ/xl decreases with increased Re at low velocities, where the flame "attaches" at the leading edge of the plate, xl=0. The standoff distance represents the distance between the solid surface and the position of the peak flame temperature at a fixed value of xl. As the air velocity is increased, the flame attachment point moves downstream and is indicated by the position of the peaks in Figure 2. The flame standoff distance at the point of attachment also decreases with increased air velocity in the computations. Downstream of the flame attachment point, the standoff distance decreases continuously with Re. It appears that the computations predict higher values of dimensionless standoff distance with increased air velocity at large values of Re. This trend appears to be in agreement with the measured values of the dimensionless standoff distance, which are also shown in Figure 2.

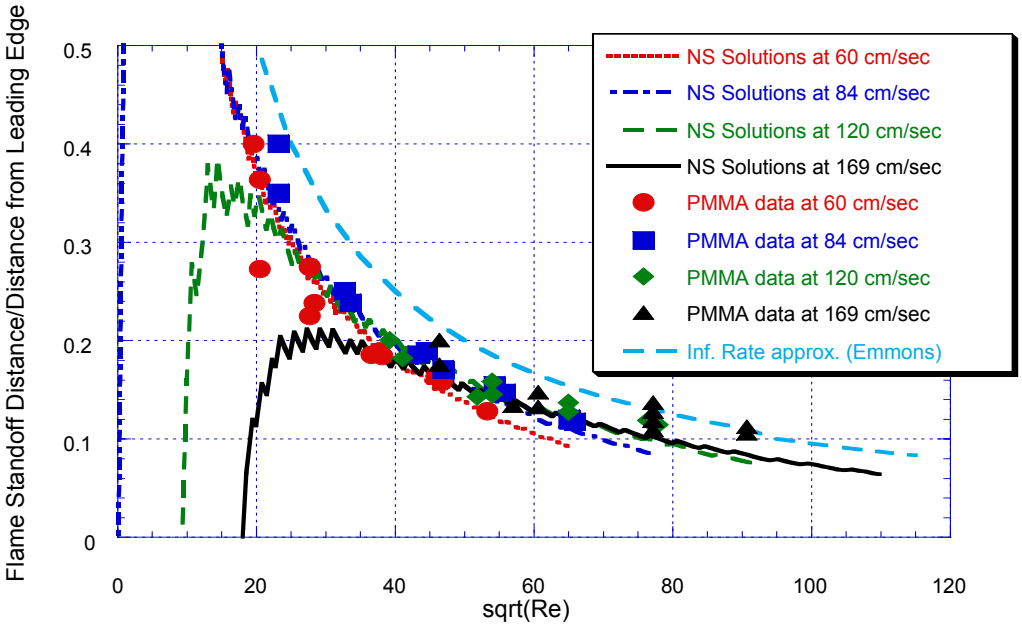

Figure 2 Comparision of NS Solutions for Flame Standoff Distance with PMMA data and the Classical Boundary Layer (BL) Theory Given by10.0/sqrt(Re)

In PMMA experiments, temperature were measured simultaneously with fine thermocouples located at different values of xl. At each value of xl, the thermocouple is moved across the flame to map the temperature profile. The location of the maximum temperature with respect to the PMMA surface was obtained from the temperature profile and is defined as the flame standoff distance. These measurements were made at about 1 minute after the sample surface has been ignited. Therefore, the surface is still flat at all values of xl. The computations seem to predict the data well at all Re.

Figure 2 also shows the classical BL solutions given by Emmons. The dimensionless standoff distance was calculated from the Nusselt number, $Nu=xl/\delta=0.1\ Re^{1/2}$. A value of 1.3 was used for B number to obtain f(0)=-0.3 in equation (54) given by F.A. Williams [31]. Clearly, the dimensionless standoff distance correlates with the single parameter Re. This is due to the neglect of finite rate combustion kinetics and axial diffusion terms in the classical BL analysis. Unlike the computations, the dimensionless flame standoff distance approach infinity in the classical BL theory as Re approaches zero. Even at air velocities of 60 and 84 cm/sec, the computations predict finite values for the standoff distance and are not shown in Figure 2. At large values of Re, the BL solutions agree with the computations and the experimental data as the axial gradients and reaction rates become small.

Figure 3 compares computational results (NS Solutions), PMMA data and the BL theory of Emmons for dimensionless regression rate Nu for air velocity, U=60 cm/sec. The NS solutions show an increase in Nu with Re. As Re increases, the flame standoff distance decreases.

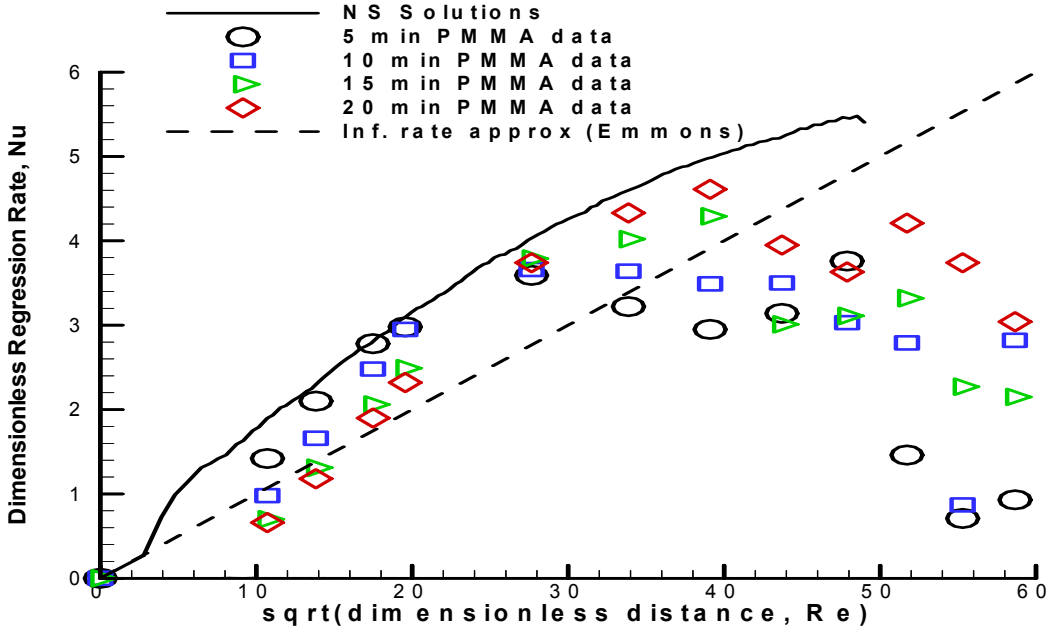

Figure 3 Comparision of Steady State NS Solutions and BL theory with PMMA Experiments Performed for Different Burn Times and at Fixed U=60 cm/sec

Therefore, the heat feedback from the flame to the surface increases and results in increased Nu. One must note that Nu multiplies r0 with xl and results in small values of Nu at small values of xl. This is despite large values of heat feed back and r0 near the leading edge, where the flame "attaches" at relatively low air velocity.

Figure 3 also shows PMMA data, which were measured at the end of 5, 10, 15 and 20 minutes burn times in different experiments. They clearly show that Nu decreases with time at small values of xl or Re, and increases with time at large values of the dimensionless distance Re. At small values of xl, flame standoff distance δ is small and regression rate r0 is high. As time progresses, the initially flat surface changes its shape and forms a valley. The depth of the valley

is the highest at the flame attachment point and decreases with xl. Also, the depth increases as time progresses from 5 to 20 minutes. It was observed that the regression rate r0 decreases as the valley deepens with time at the small values of xl due to the moving boundary effect. It was also observed that the change in shape of the surface is not significant downstream. Therefore, the computations are close to the data near the leading edge, where Re is small, at short burn time (5 min.). As time progresses the computations overpredict Nu at small value of Re since the NS solutions do not take into account the moving boundary effects. Also, the deviation between the computations and data are high close to the leading edge and decrease with increased xl or Re up to sqrt(Re)=20 due to decreasing moving boundary effects.

At large distances from the leading edge or large values of Re (sqrt(Re)>25), the data show a decrease in Nu with increased Re and result in increased deviation from the computations. Clearly, Nu increases with time at large values of Re in the experiments. The experiments show that r0 falls from about 1mm/min near the leading edge to about 0.2 mm/min at 6 cm from the leading edge. This corresponds to a drop in heat flux to the surface from 3.15 W/cm^2 to 0.63 W/cm^2 with increased xl. At these low values of heat flux downstream, it is expected that the heat transfer into the solid phase, which drives the pyrolysis process, is transient based on the flameless-pyrolysis experiments reported in literature [25]. In these experiments [25], PMMA sample was exposed to a radiant panel at constant but low values of heat flux to show that the mass loss rate increases over tens of minutes before reaching steady state. In our experiments, however, the surface was prepyrolysed; therefore, the heat-up time is expected to be small, but in-depth pyrolysis is still significant, especially at small air velocities. Indeed, when our regression data are plotted against Fourier number, $F=\alpha t/xl^2$, Nu becomes independent of time at F>1 and at all values of U. Hence, it is clear that transient conduction into the solid phase and pyrolysis increase Nu with time. The larger the value of xl or Re the larger the transient period. The computations do not account for the transient heat transport in the solid phase and overpredict the data during the transient at large values of xl. At large time, 20 min., however, the computations predict the data correctly up to sqrt(Re)=40 and the values of Nu correspond to the steady state values. For sqrt(Re)>40, the data fall below the steady state computations due to the transient solid phase effects. Clearly, Figure 3 shows that the moving boundary effects dominate near the leading edge and transient solid conduction dominate near the trailing edge of the plate, and the quasi-steady state holds in the middle region of the plate as indicated by the agreement between the data and the computations. Therefore, Figure 3 also shows spreading of the effects of valley and in-depth pyrolysis with time, and can be used to evaluate spread rates.

Figure 3 also shows BL theory that predicts a linear relationship between Nu and sqrt(Re). Like the computations, it imposes a linear relationship between the heat feedback and mass loss rate at the surface at steady state. It appears that the computations, which take into account the finite rate kinetics and axial diffusion, lead to higher values of Nu than the boundary layer theory. Clearly, BL theory under predicts the data as one approaches steady state in the experiments.

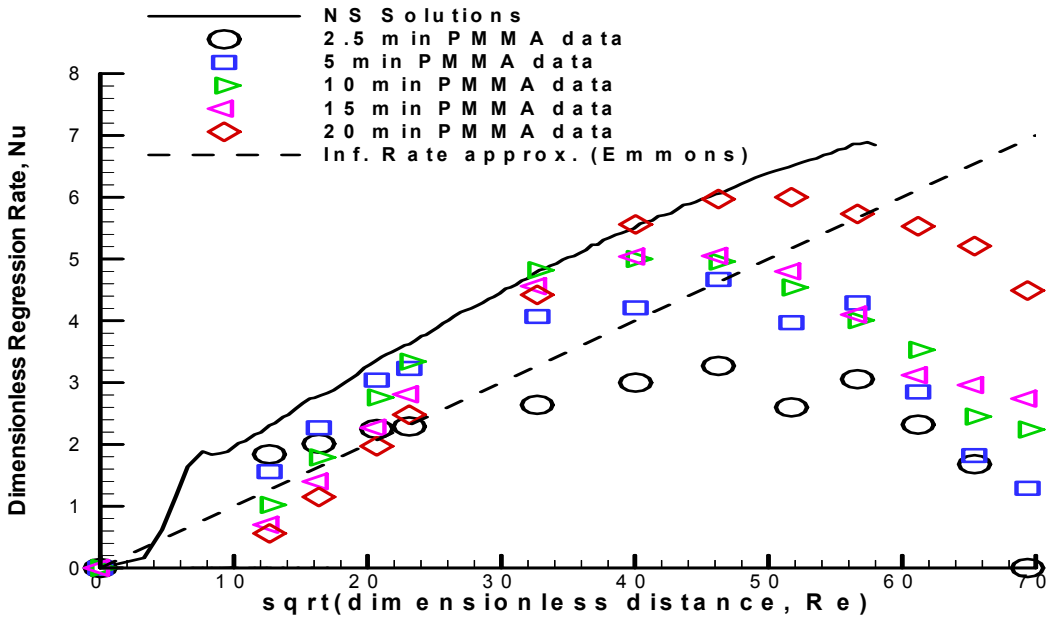

Figure 4 Comparision of Steady State NS Solutions and BL theory with PMMA Experiments Performed for Different Burn Times and at Fixed U=84 cm/sec

Figure 4 compares the computations and BL theory with the PMMA data for U=84 cm/sec. The trends shown in Figure 3 can also be seen here. At large values of Re or xl, however, the Nu predicted by computations are slightly higher at U=84 cm/sec than at U=60 cm/sec at a fixed value of Re. The data also show the same trend. One also begins to see that the data are closer

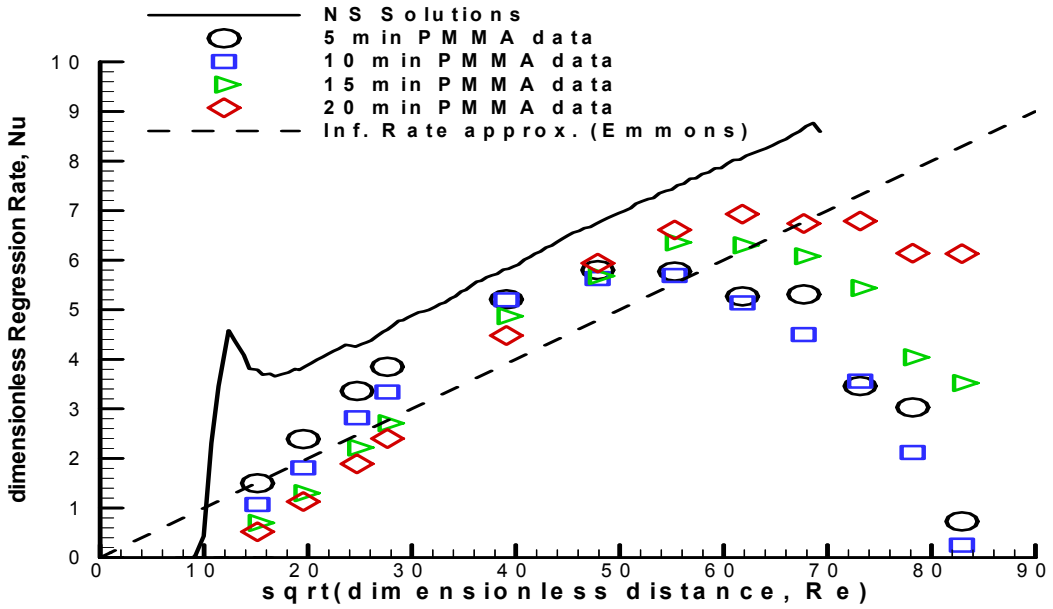

Figure 5 Comparision of Steady State NS Solutions and BL theory with PMMA Experiments Performed for Different Burn Times and at Fixed U=120 cm/sec

to the computations at large Re (say sqrt(Re)=50) for U=84 cm/sec than for U=60 cm/sec. This suggests that the transient period gets shorter as the air velocity is increased at fixed Re.

Figures 5 and 6 show computations at relatively high air velocities of 120 and 168 cm/sec, respectively. At these velocities, the flame "attaches" farther (few mm) from the leading edge of the PMMA plate both in computations and in experiments. In computations, however, the peak regression rate predicted is 4 times higher than in experiments. This discrepancy is due both to the moving boundary effects and discretization errors involved in simulating the sharp change in r0. Therefore, the NS solutions shown in Figures 5 and 6 exhibit a peak unlike the experiments. As xl or Re increases, the solutions for Nu become linear with sqrt(Re) unlike those shown in Figures 3 and 4, perhaps due to negligible axial diffusion and reaction rates.

As the velocity U is increased in Figures 3 to 6, the transient period decreases and the data get closer to the steady state computations for increased values of Re. At 20 min. burn time, the data fall below the steady state NS solutions at sqrt(Re)>40 and sqrt(Re)>100 at U=60 and 168 cm/sec respectively.

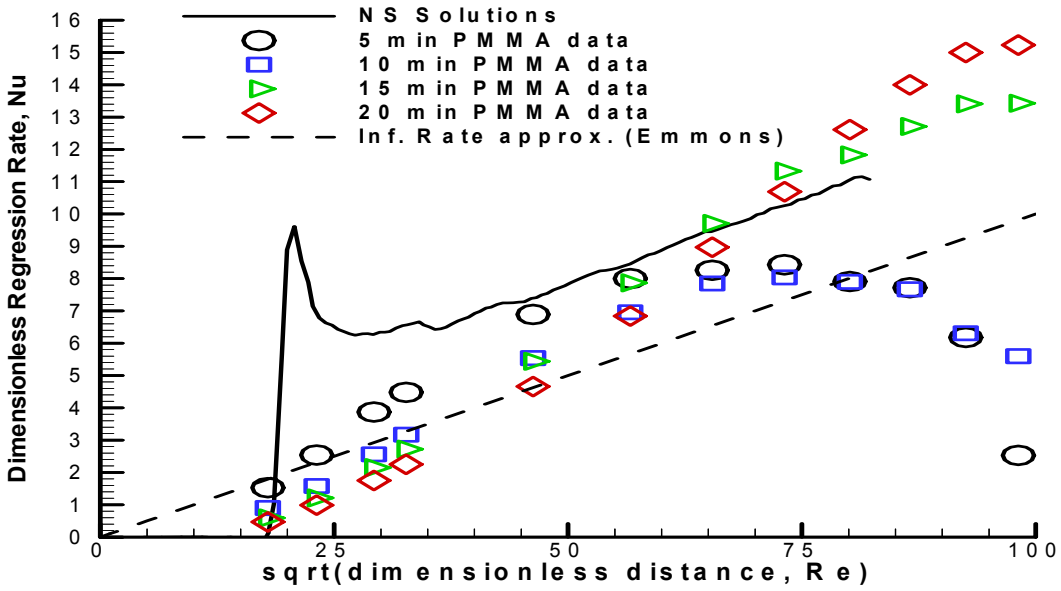

Figure 6 Comparision of Steady State NS Solutions and BL theory with PMMA Experiments Performed for Different Burn Times and at Fixed U=168 cm/sec

At U=168 cm/sec, the computations seem to underpredict the data for sqrt(Re)>75 in Figure 6. In experiments, the flame standoff distance was found to decrese with time slightly (<40%) at large values of xl. This may be due to change in boundary layer attachment position due to formation of a large valley at the high velocity and at large time. At small velocity or small time, however, the effect of valley on boundary layer attchment is expected to be small at small values of Reynolds number based on the step size (Re_{step} <1000), and the effects of transient heat conduction into the solid dominate. As expected, BL solutions do not predict flame attachment.

The BL theory is parallel to the computations and underpredict the experimental data at high values of Re.

CONCLUSIONS

Solutions of NS equations are obtained for finite rate combustion and pyrolysis and fully variable properties. They are found to agree with the experimental data for the flame standoff distance. Slightly higher values are predicted by the BL theory.

The NS solutions predict the dimensionless regression rates to increase with increased U at fixed Re, unlike the BL theory. At small values of xl or Re, the computations agree with the PMMA data for small burn time. As the burn time increases, the surface deviates from being flat and the regression rates decrease with time. The computations overpredict the regression rates as the burn time increases due to significant moving boundary effects. At large values of xl or Re, the steady state computations agree with the data for large burn times. At large values of xl, the heat flux at the surface is small and leads to significant transient effects in the solid phase. Therefore, as time progresses, the regression rates increase with time at large values of xl and reach steady state. As the air velocity is increased, the transient time reduces due to relatively high heat flux to the surface, and the steady state computations predict the data well.

ACKNOWLEDGMENTS

This work was supported by the Office of Naval Research through Naval Research Laboratory and through Code 334, Damage Control Task of FY01 BA2 Surface Ship Technology Program.

REFERENCES

(1) Beck, G.G et al., "Full Scale Machinery Space Water Mist Tests: Final Design Validation", NRL Ltr Rpt Ser 6180/0077, February, (1997)
(2) Beck, G.G., DiNenno, P.J., Hill, S.A., and Leonard, J.T., "Full-scale Testing of Water Mist Fire Extinguishing Systems for Machinery Spaces on U.S. Army Watercraft", NRL Memo Report, 6180-96-7814, 19 February, (1996)
(3) R.L. Darwin and Williams, F.W., "the Development of Water Mist Fire Protection Systems for U.S. Navy Ships", Naval Engineers Journal, **112**, November (2000)
(4) Ndubizu, C.C., Ananth, R., and Tatem, P.A., "The Effects of Droplet Size and Injection Orientation on Water Mist Suppression of Low and High Boiling Point Liquid Pool Fires"", Combustion Science & Technology, **157**, 63-86 (2000)
(5) Prasad, K., Li, C., Kailasanath, K., Ndubizu, C.C., Ananth, R., and Tatem, P.A., 'Numerical Modeling of Water Mist Suppression of Methanol Liquid Pool Diffusion Flame", Combustion Theory & Modeling , **3**, 656 (1999)
(6) Ndubizu, C.C., Ananth, R., Tatem, P.A., and Motevalli, V.., "On Water Mist Fire Suppression Mechanisms in a Gaseous Diffusion Flame", International J. of Fire & Safety (1998)
(7) Fernandez-Pello, A.C., Comb. & Flame, 36, 63 (1979)
(8) Fernandez-Pello, A.C. and Hirano, T., Comb. Sci. and Tech., 32, 1 (1983)

(9) Tewarson, A. and Ogden, S.D., Comb. & Flame, 89, 237 (1992)
(10) Tewarson, A. and Pion, R.F., Comb. & Flame, 26, 85 (1976)
(11) Emmons, H.W., Z. Angew. Math. Mech., 36, 60 (1956)
(12) Sibulkin, M., Kulkarni, A.K., and Annamalai, K., Comb. & Flame, 44, 187 (1982)
(13) Chen, C-H. and Tien, J., Comb. Sci. and Tech., 50, 283(1986)
(14) Mao, C.-P., Kodama, H., and Fernandez-Pello, A.C., Comb. & Flame, 57, 209 (1984)
(15) Kodama, H., Miyasaka, K., and Fernandez-Pello, A.C., Combust. Sci. and Tech., 54, 37(1987)
(16) Fernandez-Pello, A.C. and Williams, F.A., 15 th International Symposium on Combustion, The Combustion Institute (1974)
(17) Fernandez-Pello, A.C., Comb. & Flame, 36, 63 (1979)
(18) Zhou, L. and Fernandez-Pello, A.C., Proceedings of the Third International Symp. on Fire Safety Science, 415, (1991)
(19) Agrawal, S., Comb. Sci. and Tech., 91, 187 (1993)
(20) Ndubizu, C.C., Ananth, R , Tatem, P.A., "Experimental Investigation of a Forced Flow Boundary Layer Flame Over PMMA", The Second Joint Meeting of the U.S. Sections of the Combustion Institute, Oakland, CA, March 26-28, 2001
(21) Ananth, R., Ndubizu, C.C., Tatem, P.A., Patnaik, G., and Kailasanath, K., "Boundary-Layer Diffusion Flame Formed Over a Porous Plate", The Second Joint Meeting of the U.S. Sections of the Combustion Institute, Oakland, CA, March 26-28, 2001
(22) Ananth, R., Ndubizu, C.C., Tatem, P.A., Patnaik, G., and Kailasanath, K,"Full Navier-Stokes Modeling of a Boundary-Layer Diffusion Flame Over a Porous Flat Plate", Sixth International Microgravity Combustion Workshop, Cleveland, OH, May 22-24, (2001)
(23) Ananth, R., Ndubizu, C.C., Tatem, P.A., Patnaik, G., and Kailasanath, K, "Suppression Dynamics of a Boundary-Layer Diffusion Flame", Halon Options Technical Working Conference, Albuquerque, NM, April 24-26, (2001)
(24) Ananth, R., Ndubizu, C.C., Tatem, P.A., Patnaik, G., and Kailasanath, K., "Boundary-Layer Diffusion Flame Over a PMMA Surface", Fall Technical Meeting of the Eastern States Section of the Combustion Institute, Hilton Head, SC, December 2-5, (2001)
(25) Agrawal, S. and Atreya, A., 24 th Symposium (International) of the Combustion Institute, 1685 (1992)
(26) Seshadri, K. and Williams, F.A., J. Polym. Sci., 16, 1755 (1978)
(27) Tewarson, A., SFPE Handbook of Fire Protection Engineering, Second Edition, Chapter 3 (1995)
(28) Arisawa, H. and Brill, T.B., Comb. & Flame, 109, 415 (1997)
(29) Ananth, R., Ndubizu, C.C., Tatem, P.A., "A Numerical Model for the Development of a Boundary Layer Diffusion Flame Over a Porous Flat Plate", NRL Memorandum Report NRL/MR/6183--01-8547, Naval Research Laboratory, Washington, DC, April 23, (2001)
(30) Patnaik, G., Laskey, K.J., Kailasanath, K., Oran, E.S., and Brun, T.A., "FLIC-A Detailed, Two Dimensional Flame Model", NRL Memorandum Report 6555, Naval Research Laboratory, Washington, DC, September 27, (1989)
(31) Williams, F.A., "Combustion Theory", 2 nd Edition, Addison-Wesley Pub. Co., Redwood City, CA (1985)